

DESIGN OF HIGHLY-SENSITIVE CURRENT MONITOR WITH HTS SQUID AND HTS MAGNETIC SHIELD

T. Watanabe, S. Watanabe, T. Ikeda, M. Kase T. Katayama, RIKEN, Wako, Saitama, Japan
T. Kawaguchi, KT Science Ltd., Kakogawa, Hyogo, Japan

Abstract

A high-temperature superconducting (HTS) magnetic shield based on $\text{Bi(Pb)}_2\text{-Sr}_2\text{-Ca}_2\text{-Cu}_3\text{-O}_x$ (Bi-2223) was fabricated by plasma spraying for the purpose of observing a somatosensory-evoked magnetic field generated from the human brain[1]. Recently, a Bi-2223 cylindrical magnetic shield was developed by dip-coating on a 99.9 % MgO ceramic substrate. A highly-sensitive current monitor using this HTS magnetic shield in combination with a HTS Superconducting QUantum Interference Device (SQUID) is being developed in the RIKEN RI beam factory for high-accuracy nondestructive measurement of faint beams such as a radioisotope beam.

1 INTRODUCTION

A DC current transformer (DCCT) based on the second-harmonic modulator-demodulator has been used in a circular ring, the sensitivity of which is about $1 \mu\text{A}$ [2]. In order to measure a beam intensity less than $0.1 \mu\text{A}$, current transformers using the principle of a low temperature superconducting (LTS) cryogenic current comparator (CCC) had been developed [3] [4]. On the other hand, a prototype HTS CCC with an HTS gradiometer SQUID has been successfully demonstrated as a means of nondestructive sensing of argon beams in the current range of $1 - 20 \mu\text{A}$ [5]. The HTS technology enables us to develop a system equipped with a highly-sensitive current monitor with HTS SQUID and a HTS magnetic shield. This paper describes the system design and the present status of the monitor.

2 PRINCIPLE OF HTS CCC

The principle of superconductive CCC is based on the property of the Meissner effect of superconducting materials. A schematic drawing of the superconductive CCC that we are designing is shown in Fig. 1(a). The MgO ceramic tube as a substrate of the HTS magnetic shield is coated on both sides, inside and outside, with a thin ($300 \mu\text{m}$) HTS material. When the charged particle (ion or electron) beam is being passed along the axis of a HTS tube, a shielding current produced by the Meissner effect flows in the opposite direction along the wall of the HTS tube so as to screen the magnetic field generated by the beam. Since the outer surface is designed to have a bridge circuit (Fig. 1), the current generated by the charged particle beam concentrates on the bridge circuit and forms an azimuthal magnetic field Φ around the bridge circuit. Moreover, the HTS SQUID is close to the bridge circuit and the

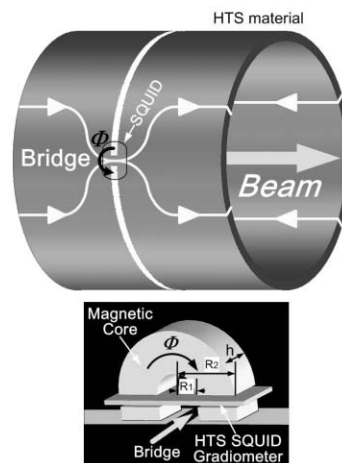


Figure 1: (a) Schematic drawing of the superconductive CCC that we are designing. (b) Structure of the SQUID gradiometer and the magnetic core near the bridge.

HTS SQUID can detect the azimuthal magnetic field with a high S/N ratio. In particular, since the SQUID gradiometer has two pickup coils that are wound in opposite directions and connected in series, the signal level is expected to be improved by a factor 2, while an background noise can then be greatly reduced more than 40dB. Furthermore, to obtain a higher coupling efficiency, we consider the possibility of introducing the high-permeability magnetic core in the HTS CCC. The sketch (Fig. 1 (b)) represents the structure of the SQUID gradiometer and the magnetic core near the bridge.

3 HTS SQUID SYSTEM

Fig. 2 shows the characteristics of HTS SQUID magnetometer that was used to measure the field distribution inside a HTS magnetic shield [6]; (a) current (x-axis) vs. voltage (y-axis) appears across the Josephson junctions of the HTS SQUID, (b) the relationship of the magnetic field B (x-axis) at the input coil with voltage (y-axis). The response of the sensitive SQUID loop is periodic with respect to a magnetic flux quantum, $\Phi_0 = h/2e = 2.068 \times 10^{-15} \text{ weber}$. Then a flux-locked loop method is usually used in the HTS SQUID circuit because a wide dynamic range and a high resolution of the flux sensitivity are required. Fig. 3 shows the circuit diagram of the HTS DC SQUID (2 Josephson Junction) and flux-locked loop. The region in the box is kept below critical temperature T_c . The

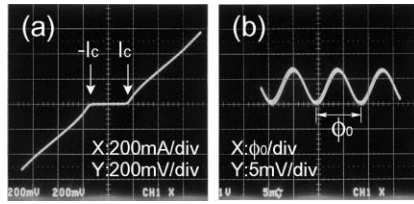


Figure 2: Characteristics of SQUID. (a) current (x-axis) vs. voltage (y-axis) appears across the Josephson junctions of HTS SQUID, (b) relationship of the magnetic field B (x-axis) at the input coil with voltage (y-axis).

magnetic flux density B induced by the charged particle beam is transferred to the HTS SQUID with the aid of the pickup coil and the input coil, which are built-in in the HTS SQUID itself. The flux-locked loop can make a linear operation with respect to the HTS SQUID circuit because it cancels the external magnetic flux density B , with the aid of the bias current flowing in the feedback coil as shown in Fig. 3. Modulation and synchronous detector are used to create a flux-locked loop circuit similar to negative feedback phase-locked circuit. The voltage appearing in the resistance, if it appears in the figure, is measured in order to obtain the calibrated shield current, namely, the beam current passing through the HTS tube.

The HTS DC SQUID system which is composed of HTS SQUID gradiometer ($Y\text{-Ba}_2\text{-Cu}_3\text{O}_{7-\delta}$), cryogenic cable, flux-locked loop module, a fiber-optic composite cable that connects the flux-locked loop module to the control electronics and a set of control electronics and that system is commercially available [7]. The heater is mounted close to the SQUID chip in the sensor package in order to purge any magnetic flux trapped in the sensor. The fiber-optic composite cable is used to eliminate grounding and shielding problems that often affect SQUID electronics. The HTS DC SQUID system is shown in Fig. 4 and the specifications of the system are tabulated in Table 1. Fig. 5 measured noise spectrum in frequency domain shows a $1/f$ noise structure and a noise level is very low compared with the conventional HTS SQUID.

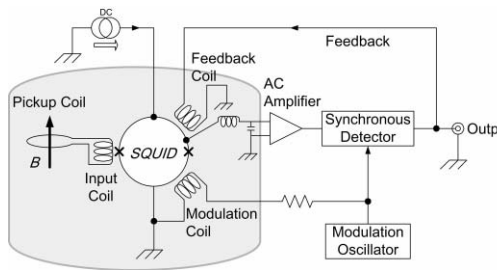


Figure 3: Circuit diagram of a HTS DC SQUID (2 Josephson Junction) and flux-locked loop. The region in the box is kept below critical temperature T_c .

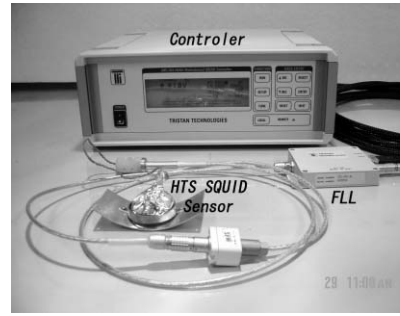


Figure 4: The HTS DC SQUID system Model BMS-G with HTG-10R.

Table 1: The specifications of the HTS DC SQUID system.

Noise level	34 fT / \sqrt{Hz} @ 5kHz
Operation temperature	77 K
Feedback gain	1, 2, 5, 10, 20, 50, 100, 200, 500
High pass filter	DC, 0.3 Hz
Low pass filter	5 Hz, 200 Hz, 2kHz, 20kHz
Date accuracy (AD)	16 bit
Date acquisition rates	20000 words/s
Remote control	IEEE-488, RS-232

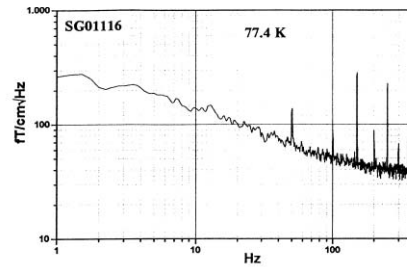


Figure 5: The measured noise spectrum in frequency domain shows a $1/f$ noise structure and a noise level is very low compared with the conventional HTS SQUID.

4 HTS MAGNETIC SHIELD

The examination of the HTS magnetic shield coated on the MgO substrate had been proceeding step by step. The critical current (I_c) and critical temperature (T_c) of the Bi-2223 cylindrical HTS shield should be confirmed to obtain a stable HTS CCC. By a DC four-probe method using a small piece of Bi-2223, I_c of 4500A/cm² and T_c of 106 K were acquired. Furthermore, X-ray diffraction analysis has been used to identify the formation of the Bi-2223 phase. After the above-mentioned tests, in order to measure the field distribution inside the HTS magnetic shield and to obtain the attenuation factor, we constructed the measurement system [6]. From now on, we define a direction of the cylindrical axis as the z-direction and a direction perpendicular to the axis as the x-direction. And an attenuation factor is defined by dividing the magnetic field inside the shield by an external magnetic field. By those measure-

ments, the attenuation factor of 5×10^{-4} in the z-direction and that of 8×10^{-2} in the x-direction were obtained. Then if the magnetic shield is reinforced by three-layer permalloy shield which has 1/500 of shielding factor, 3×10^{-5} T of geomagnetism will be decreased to 4×10^{-14} T in the z-direction and 8×10^{-12} T in the z-direction, since SQUID gradiometer has -50dB of shielding factor.

5 PROTOTYPE OF HTS CCC

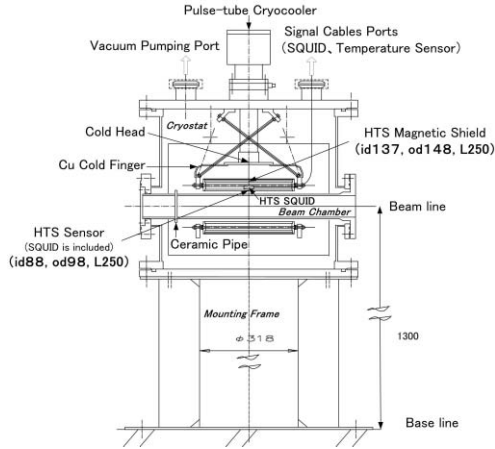


Figure 6: Schematic drawing of a prototype of highly-sensitive current monitor with HTS SQUID and HTS magnetic shield.

We are constructing a prototype of highly-sensitive current monitor with a HTS SQUID and HTS magnetic shield and the schematic drawing is shown in Fig. 6. The HTS magnetic shield and the HTS current sensor includes the HTS SQUID are cooled by a pulse-tube cryocooler which is a very low vibration type and has a refrigeration power of 11W. We had already tested the vacuum and the pulse-tube cryocooler system. While the pulse-tube cryocooler is capable of lower temperatures than that of liquid nitrogen, the limited operating range of the HTS SQUID used required operation between 72 K and 77 K. Furthermore it is necessary to stabilize the HTS SQUID to better than 1 mK by using a cryogenic temperature control which has a temperature sensor of four channels and a heater.

6 FUTURE PLAN

In order to improve coupling efficiency between the SQUID sensor and the magnetic field generated by the beam, we are considering the possibility of introducing the high-permeability magnetic core in the HTS CCC (see Fig. 1). Fig. 7 shows the result of the magnetic field calculation by the MAD program and Fig. 8 plots the z-component of magnetic field B_z between two cores in accordance with x axis. This calculation shows that a signal was improved about 290 times, when the high-permeability magnetic core is used.

We are planning to install a prototype of highly-sensitive current monitor with a HTS SQUID and HTS magnetic

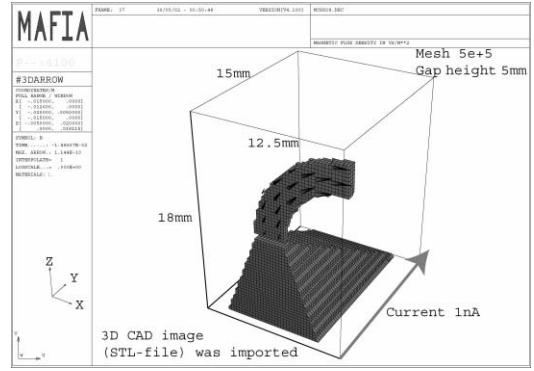


Figure 7: The result of the magnetic field calculation by the MAD program when the high-permeability magnetic core is used.

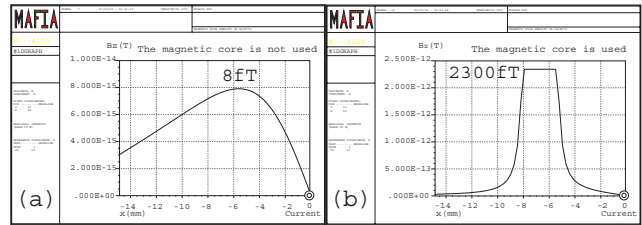


Figure 8: Plots of the z-component of magnetic field B_z between two cores in accordance with x axis. This calculation showed that a signal was improved about 290 times, when the high-permeability magnetic core was used.

shield in the beam transport line of the RIKEN Ring Cyclotron (RRC) to measure the beam current by this summer.

7 ACKNOWLEDGMENTS

The authors thank Robert L. Fagaly of Tristan Technologies for valuable discussions on the HTS SQUID system. They thank S. Ono of Central Research Inst. of Electric Power Industry and Y. Yoshida of National Inst. for Materials Sci. for valuable discussions on the HTS magnetic shield.

8 REFERENCES

- [1] H. Ohta et al.: IEEE Trans. on Appl. Supercond., Vol. 9, No.2, 1999-6, p. 4073.
- [2] K. Unser: IEEE Trans.Nucl.Sci. 28, 1981, p. 2344.
- [3] A. Peters et al.: Proc. 5th European Particle Acc. Conf., Barcelona, 1996 - 6, p. 1627.
- [4] T. Tanabe et al.: Proc. 6th European Particle Acc. Conf., Stockholm, 1998 - 6, p. 1610.
- [5] L. Hao et al.: IEEE Trans. on Appl. Supercond. (ASC2000), Vol. 11, No.1, 2001-3, p. 635.
- [6] S. Watanabe et al. : This conference.
- [7] Model BMS-G with HTG-10R manufactured by TRISTAN TECHNOLOGIES.